International Journal of Automotive Technology, Vol. 10, No. 3, pp. 285–295 (2009)
DOI 10.1007/s12239–009–0033–1

1229–9138/2009/046–03

INFLUENCE OF INJECTION PARAMETERS ON THE TRANSITION FROM PCCI COMBUSTION TO DIFFUSION COMBUSTION IN A SMALL-BORE HSDI DIESEL ENGINE

T. FANG[1)*], R. E. COVERDILL[2)], C.-F. F. LEE[2)] and R. A. WHITE[2)]

[1)]Department of Mechanical and Aerospace Engineering, North Carolina State University, 3182 Broughton Hall-Campus Box 7910, 2601 Stinson Drive, Raleigh, NC 27695, USA
[2)]Department of Mechanical Science and Engineering, University of Illinois at Urbana-Champaign, 1206 West Green Street, Urbana, IL 61801, USA

(Received 11 June 2008; Revised 13 October 2008)

ABSTRACT–In this paper, the influence of injection parameters on the transition from Premixed Charge Combustion Ignition (PCCI) combustion to conventional diesel combustion was investigated in an optically accessible High-Speed Direct-Injection (HSDI) diesel engine using multiple injection strategies. The heat release characteristics were analyzed using in-cylinder pressure for different operating conditions. The whole cycle combustion process was visualized with a high-speed video camera by simultaneously capturing the natural flame luminosity from both the bottom of the optical piston and the side window, showing the three dimensional combustion structure within the combustion chamber. Eight operating conditions were selected to address the influences of injection pressure, injection timing, and fuel quantity of the first injection on the development of second injection combustion. For some cases with early first injection timing and a small fuel quantity, no liquid fuel is found when luminous flame points appear, which shows that premixed combustion occurs for these cases. However, with the increase of first injection fuel quantity and retardation of the first injection timing, the combustion mode transitions from PCCI combustion to diffusion flame combustion, with liquid fuel being injected into the hot flame. The observed combustion phenomena are mainly determined by the ambient temperature and pressure at the start of the second injection event. The start-of-injection ambient conditions are greatly influenced by the first injection timing, fuel quantity, and injection pressure. Small fuel quantity and early injection timing of the first injection event and high injection pressure are preferable for low sooting combustion.

KEY WORDS : HSDI diesel engine, Conventional diesel combustion, PCCI combustion

1. INTRODUCTION

Because of the increasing threat of limited fossil fuel resources and the worldwide concern of environmental issues, emissions regulations for current engines are becoming increasingly more stringent. Direct Injection (DI) diesel engines are attractive power sources due to their superior fuel economy and excellent reliability. However, oxides of nitrogen (NOx) and Particulate Matter (PM) must be reduced for diesel engines to meet the stricter emissions standards. New techniques and combustion concepts have been developed to solve the problems.

Homogeneous Charge Compression Ignition (HCCI) combustion is a promising technique that provides a unique approach to simultaneously reduce NOx and PM emissions while maintaining high thermal efficiency. For HCCI combustion, a premixed or ideally homogeneous air-fuel mixture auto-ignites due to compression; it is a bulk combustion, eliminating local high temperature regions. Consequently, the NOx emissions are extremely low compared with conventional diesel combustion and Spark Ignition (SI) combustion. In addition, because the air-fuel mixture is premixed, there is no locally rich region, so soot and PM are also greatly reduced. Early studies of the HCCI combustion mode were carried out in two-stroke engines (Onishi *et al*., 1979; Noguchi *et al*., 1979) and in four-stroke engines (Najt and Foster, 1983; Thring, 1989) by using heavy Exhaust Gas Recirculation (EGR). It was shown that, in the HCCI combustion mode, the ignition process is controlled by low temperature (950 K) hydrocarbon oxidation kinetics, while the energy release process is controlled by high temperature (above 1000K) hydrocarbon oxidation.

Multiple injection strategies have been reported for simultaneous reduction of NOx and PM in both large bore DI diesel engines (Nehmer *et al*., 1994; Tow *et al*., 1994; Han *et al*., 1996) and small-bore high-speed DI diesel engines (Zhang, 1999; Tanaka *et al*., 2002; Chen, 2000). Several studies (Nehmer and Reitz, 1994; Tow *et al*., 1994; Han *et al*., 1996) have shown that pulsed injections may

**Corresponding author.* e-mail: tfang2@ncsu.edu

provide a method to reduce PM emissions and allow for the reduction of NOx from controlled pressure rise. Late injection in double or triple injection strategies can promote the particulate oxidation process. Reduced soot emissions are due to the fact that soot-producing rich regions are not replenished when the injection pulse is terminated and restarted. The combustion mode in these studies can be categorized as conventional diesel combustion. In addition to the studies in heavy duty DI diesel engines, investigations have also been performed in small-bore HSDI diesel engines using multiple injection strategies. The effects of pilot injection on the combustion process were studied experimentally by Zhang (1999) and Tanaka *et al.* (2002). Simultaneous reduction of combustion noise and emissions is possible by decreasing the influence of pilot burned gas through minimizing the fuel quantity and advancing the injection timing of the pilot injection. Simultaneous reduction of NOx and PM by using multiple injections was implemented in a small diesel engine (Chen, 2000) by optimizing the combinations of EGR rate, pilot timing and quantity, main timing, and dwell between the main and pilot injections. Post injection was shown to be effective in reducing PM due to the improved particulate oxidation process. In the results of these papers, the combustion modes were not limited to conventional diesel combustion. Some evidence of the PCCI combustion mode can be found in the heat release rate curves. Some results (Tanaka *et al*., 2002) were similar to the UNIBUS combustion mode using double injections, as discussed in the following sections.

Hashizume *et al*. (1998) proposed an HCCI solution for higher load operating conditions. The combustion is named MULtiple stage DIesel Combustion (MULDIC) on the basis of the PREmixed lean DIesel Combustion (PREDIC) concept (Takeda *et al*., 1996). The first stage is premixed lean combustion (PREDIC), and the second stage is diffusion combustion under high temperature and low oxygen conditions. Smoke and NOx were reduced by MULDIC even at an excess air ratio of 1.4. Further studies on the MULDIC concept were done in the same research group by Akagawa *et al*. (1999). In this study, they developed a new pintle type injector for reduced fuel penetration, especially for the early injection. The top-land crevice volume, namely the wall quenching volume, was also reduced. The results showed reductions of THC and CO emissions. At the same time, NOx and smoke can also be reduced at high load conditions.

A multi-pulse injection strategy was used by Su *et al*. (2003) in their study of HCCI combustion in an HSDI diesel engine. They used multiple short injection pulses for the early injection or followed by a main injection near Top Dead Center (TDC). When the load is less than 9.3 bar Indicated Mean Effective Pressure(IMEP), reductions of both smoke and NOx were obtained. HCCI combustion in a small bore HSDI diesel engine was also investigated using early multiple short injection pulses during the compression stroke by Helmantel and Denbratt (2004). In order to decrease the fuel wall impingement, a small-included angle injector was used. The results showed a dramatic reduction of NOx. Smoke emissions also showed a significant reduction, while HC and CO emissions substantially increased.

Investigations by Hasegawa and Yanagihara (2003) employed two injections in the HCCI combustion mode, referred as UNIform BUlky combustion System (UNIBUS). The first injection was used as an early injection for early fuel mixing and to advance the changing of fuel to lower hydrocarbons, while the second injection was used as an ignition trigger. Bulk combustion was observed in the combustion chamber. Low NOx and smoke were possible in both injections using this combustion concept. Another two-stage diesel fuel injection HCCI combustion study was done in a single cylinder small diesel engine (Kook and Bae, 2004). A large fraction of fuel was injected early during the compression stroke or even during the induction stroke. A second injection with a small amount of fuel was injected near the compression TDC to ignite all of the air-fuel mixture. The experimental results showed that the second injection could only be used as a combustion trigger for low intake air temperature. The first injection timing should be advanced earlier than 100 CAD BTDC to achieve homogeneous and non-luminous combustion. NOx was greatly reduced using this injection strategy. HC, CO, and fuel consumption were higher than in conventional diesel combustion.

Conceptually speaking, HCCI combustion is an ideal operation mode for low emission diesel engines (Choi *et al*., 2004). However, in a real diesel engine, it is quite difficult to homogeneously mix air and fuel using in-cylinder direct injection strategies, even with a very early injection during the suction stroke (Swami Nathan *et al*., 2007). A heterogenous premixed charge often occurs under these injection strategies. Mixture heterogeneity often exists, even for very early in-cylinder injection timings. In general, Premixed Charge Compression Ignition (PCCI) combustion is a more accurate terminology for these conditions than "HCCI". PCCI only requires a premixed charge, and the mixture is not required to be homogeneous. "PCCI" is a broader concept than "HCCI". Most of the above mentioned combustion modes are types of PCCI combustion.

In these previous studies, the combustion processes were often visualized through an optical engine with modified piston geometries. The replacement of the true piston shape changes the flow field into which the fuel is injected. In this work, the investigation uses an optical engine with a realistic piston geometry. Among the current operating conditions, a transition from PCCI combustion mode to conventional diesel combustion mode was seen for the second main injection. The influential factors such as injection pressure, injection timing, and injection fuel quantities are studied and the effects of the first injection parameters on the combustion mode for the second injection are addressed.

2. OPTICAL ENGINE AND FACILITY

A single-cylinder DIATA research engine supplied by Ford Motor Company was modified into the optical engine used for the current experimentation. Key aspects of the DIATA engine are listed in Table 1. Optical access to the combustion chamber was attained through the side window or through the fused silica piston top. The optical engine design maintains the geometry of the ports and combustion chamber of the original engine. A complete description of the optical engine can be found in a previous publication (Mathews *et al*., 2002). A Bosch common-rail electronic injection system was used, and was capable of injection pressures up to 1350 bar. A valve covered orifice injector with six 0.124 mm holes placed symmetrically in the nozzle tip and a spray cone angle of 150 degrees were used. The injector was fitted with a needle lift sensor monitoring the needle operation throughout injection. A Phantom v7.0 high-speed digital video camera was used to capture the natural flame emission for the whole cycle. National Instruments LabView version 6.0 was used as the data acquisition and timing control software. An optical shaft encoder with 0.25 crank angle resolution was used to provide the time basis. The engine temperatures and pressures were monitored through a multifunction data acquisition board.

3. ENGINE OPERATING CONDITIONS

The results presented in this paper are based on operating conditions considered typical for this engine. Intake temperatures and pressures were increased to match the TDC conditions of the metal engine with the same geometry and operating conditions. The operating conditions are summarized in Table 2. The fuel quantities of the first injections were calibrated and injected at given injection timings. The main injection pulse durations were adjusted to match the load for all of the cases to be 5.0 bar IMEP. The injection timing of the main injection was set at TDC for all of the cases. The fuel used was a low-sulfur European Diesel fuel, selected properties of which are shown in Table 3. Due to the extensive optical access provided by the optical DIATA engine, 3-D like combustion imaging was feasible (Fang *et al*., 2005, 2006, 2007, 2008; Miles, 2000). Combustion images were obtained using the high-speed video camera by setting the operating frame rate at 12000 frames per second with the resolution at 512×256 to capture the images from the bottom and side. For all of the cases, the exposure time was 2 ms.

Table 1. Specifications of the single cylinder DIATA research engine.

Bore	70 mm
Stroke	78 mm
Displacement/Cylinder	300 cc
Compression ratio	19.5:1
Swirl ratio	2.5
Valves/Cylinder	4
Intake valve diameter	24 mm
Ex. valve diameter	21 mm
Maximum valve lift	7.30/7.67 mm (Intake/Exhaust)
Intake valve opening	13 CAD ATDC (at 1 mm valve lift)
Intake valve closing	20 CAD ABDC (at 1 mm valve lift)
Ex. valve opening	33 CAD BBDC (at 1 mm valve lift)
Exhaust valve closing	18 CAD BTDC (at 1 mm valve lift)

Table 2. Summary of engine operating conditions.

Case number	Rail pressure [bar]	First timing [CAD ATDC]	Pilot quantity [mm^3]	Main injection timing [CAD ATDC]	IMEP [bar]
1	600	−40	0.8	0	5.05
2	600	−30	0.8	0	4.99
3	600	−40	1.3	0	5.08
4	600	−30	1.3	0	5.01
5	1000	−40	0.8	0	4.94
6	1000	−30	0.8	0	5.08
7	1000	−40	1.3	0	5.09
8	1000	−30	1.3	0	5.07

Table 3. Selected properties of the low-sulfur European diesel fuel used during experimentation.

Specific gravity	0.8352
Cetane number	52.9
Sulfur, ppm	27.5
Mid boiling point, °C	260

4. RESULTS AND DISCUSSIONS

4.1. In-cylinder Pressure and Heat Release Analysis

The optical engine was warmed up by circulating heated coolant and lubricating oil to simulate a warm engine environment. The engine operated in skip fire mode in order to reduce the heat load of the quartz piston, with one injection cycle followed by 12 motoring cycles. Pressure data were recorded and saved to the computer for post processing.

Pressure traces for the eight cases are shown in Figures 1a and 2a. In the plots, 360 CAD corresponds to the compression Top Dead Center (TDC). It is seen from the figures that high injection pressure results in faster combustion, and thus more rapid pressure increase, due to better fuel spray atomization and mixing. Combustion noise, which is directly relevant to pressure rise rate, will be higher for the higher injection pressure cases. Some knock-like combustion behaviors are seen for the high injection

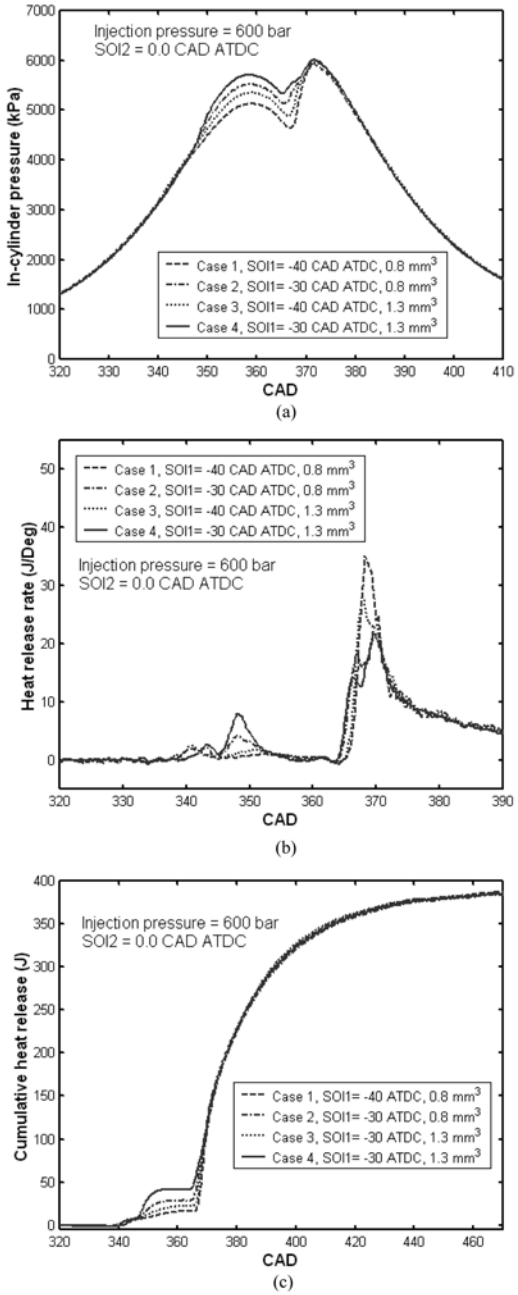

Figure 1. In-cylinder pressures (a), heat release rates (b), and cumulative heat release (c) for Cases 1~4.

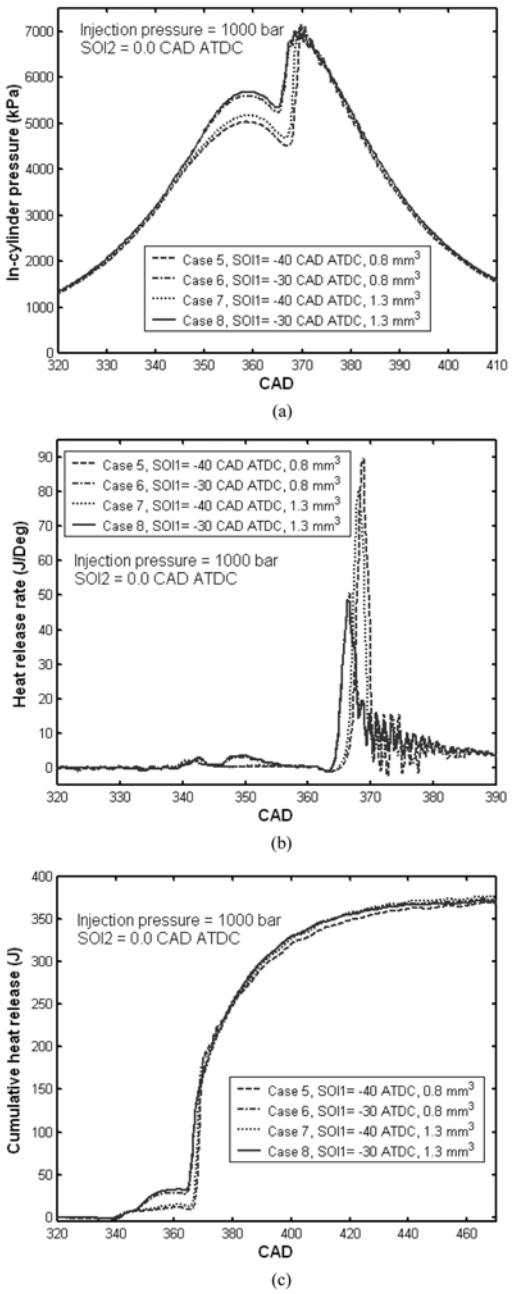

Figure 2. In-cylinder pressures (a), heat release rates (b), and cumulative heat release (c) for Cases 5~8.

pressure cases. Higher in-cylinder pressure peaks are seen for Cases 5~8 than for Cases 1~4. Earlier first injection timing and small fuel quantity lead to a longer ignition delay for the second injection. Long ignition delay for the second injection results in higher pressure increase rate and therefore higher combustion noise.

The heat release rates are illustrated in Figures 1(b) and 2(b). Results of the heat release rates support the observations in the in-cylinder pressure plots. Ignition delays are seen to be shorter for higher first fuel quantity and later first injection timing. Narrower and higher heat release peaks are observed for the higher injection pressure cases, showing more rapid combustion and concentrated heat release processes, while flatter and broader heat release rate patterns are seen for the lower injection pressure cases. For the second injection combustion, it is seen that some of the high injection pressure cases are close to PCCI combustion. However, for the low injection pressure cases, diffusion combustion becomes more apparent, with increasing first injection fuel quantity and decreasing retarding first injection timing. The combustion mode transition from diffusion combustion to PCCI combustion is observed in

Table 4. Released heats for the eight operating conditions.

Case number	First cumulative heat release [J]	Second cumulative heat release [J]	Total cumulative heat release [J]
1	15.82	372.24	388.06
2	28.43	357.24	385.67
3	21.96	365.07	387.03
4	41.19	345.14	386.33
5	11.29	359.42	370.71
6	28.39	345.28	373.67
7	14.69	363.90	378.59
8	32.29	339.55	371.84

the cases investigated.

The cumulative heat release curves for these cases are illustrated in Figures 1(c) and 2(c). The released heats of each injection are shown in Table 4. The total heat release for the low injection pressure cases is about 386~388 joules, while for high injection pressure cases, it is about 371~379 joules. Since the work outputs for these cases are similar based on the load match, lower energy input indicates higher cycle efficiency. Because the high injection pressure cases have fast burns more like constant-volume combustion than the low injection pressure cases, the cycle thermal efficiency for high injection pressure is generally higher than that of the low injection pressure cases. The released heats for the first injection show large differences for different first injection parameters. Table 4 shows that early injection timing and higher injection pressure result in less complete combustion for the first injection, which leads to lower in-cylinder temperature and pressure at the start of the second injection. The combustion mode of the second injection depends on the ambient temperature and pressure at the start of injection. Therefore, the combustion mode of the second injection greatly depends on the first injection parameters.

The in-cylinder temperature is estimated based on the intake condition and in-cylinder pressure using the ideal gas law. Some critical temperatures for the eight cases are shown in Figure 3. It is found that higher injection pressure results in lower in-cylinder temperature at the start of the second injection. The temperature is lower for early first injection timing and smaller first fuel quantity. These observations are consistent with the heat release analysis. The in-cylinder temperature at the start of the second injection event influences the ignition delay. A high temperature leads to a short ignition delay, which causes the overlap of the liquid jet with the hot flame, namely typical diffusion combustion. For the lower ambient temperature and higher injection pressure of the second injection, the combustion mode is close to PCCI combustion with little evidence of diffusion combustion. With the increase of ambient temperature, the diffusion flame becomes more pronounced, as shown in the heat release rate of the low injection pressure cases. The maximum in-cylinder bulk temperatures are

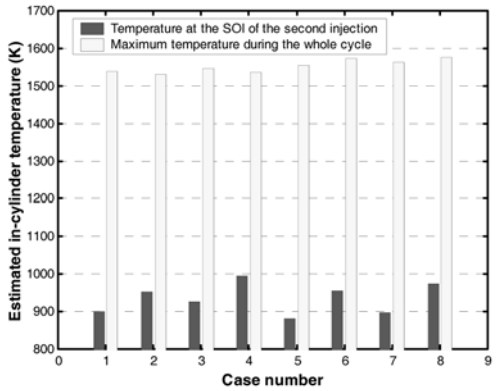

Figure 3. Estimated bulk in-cylinder temperature.

quite similar for all of the cases. Slightly higher values can be found for high injection pressures due to the faster burning process (Van Gerpen *et al.*, 1985; Kobayashi *et al.*, 1992).

4.2. Flame Luminosity

The combustion process was visualized using the high-speed video camera described in Section 2. The bottom view combustion images were used to compute the flame luminosity by summing the pixel values. For each case, 5 sets of combustion movies were taken and the flame luminosities were obtained by averaging the 5 sets of data.

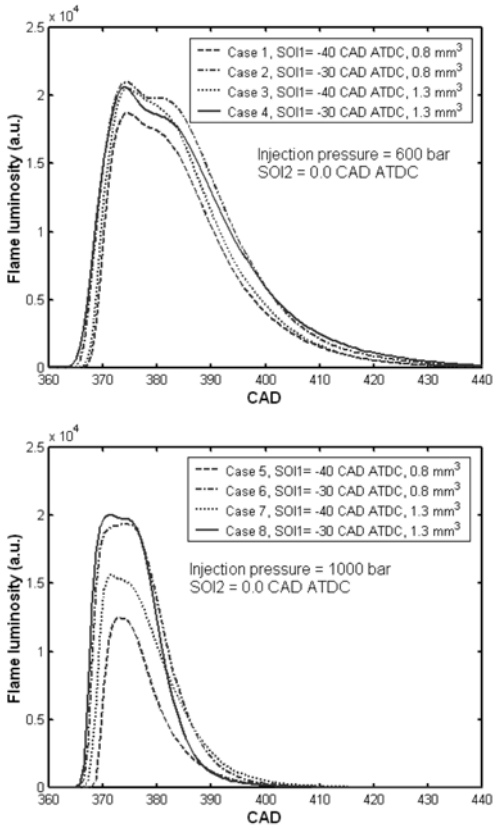

Figure 4. Flame luminosity time history for the eight cases.

The time histories of flame luminosity for the eight cases are illustrated in Figure 4. For low injection pressure, it is found that the flame luminosity curves for the four cases are similar, with long tails. These long tails are believed to be due to a slow post soot oxidation process. Similar observations for high injection pressure cases can be seen for Cases 6 and 8, while Case 5 and 7 have different flame luminosity characteristics. The flame luminosity is mainly dependent on temperature and soot concentration. Under similar temperature distributions, higher flame luminosity indicates higher soot formation. Cases 5 and 7 have much lower flame luminosity than other cases, showing low sooting and/or low temperature combustion for these two cases. The combustion duration is longer for low injection pressure cases because of reduced mixing and the slow post oxidation process.

The derivatives of flame luminosity are shown in Figure 5 and, to some extent, show the soot formation rate and oxidation rate during the combustion process. In general, higher positive peaks can be seen in the plots for the high injection pressure cases, showing faster combustion and soot formation processes. The duration for the positive flame luminosity increase rate is shorter for the high injection pressure cases. However, the negative peaks are much higher for the high injection pressure cases, indicating a higher soot oxidation rate for these cases. The negative peak timings are quite close to the maximum in-

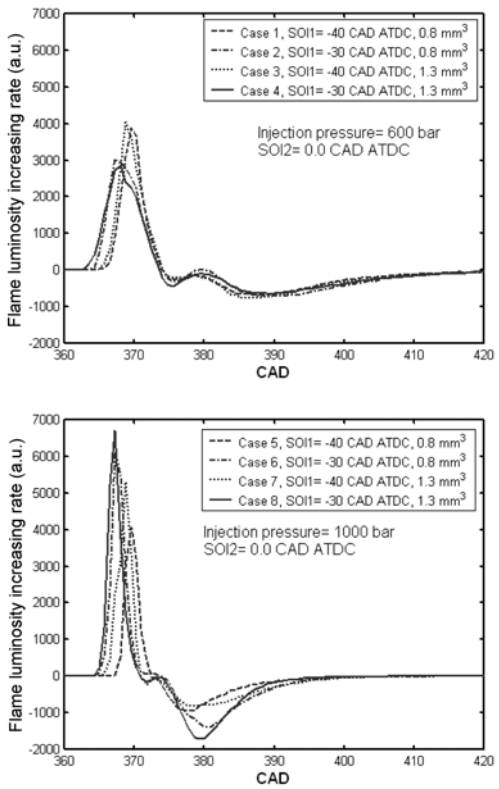

Figure 5. Rates of flame luminosity increase for the eight cases.

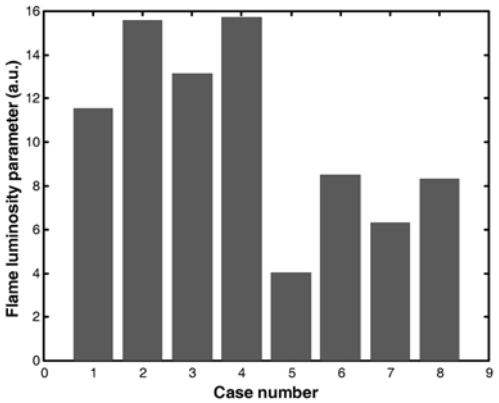

Figure 6. Flame luminosity parameter for the eight cases.

cylinder temperature timings. This confirms that a higher temperature results in a higher soot oxidation rate. It is interesting to note that Case 5, namely the typical PCCI combustion case, shows a lower increasing rate and relatively lower oxidation rate, which indicates that premixed combustion has a lower soot formation rate with less fuel rich regions.

Using the same logic as in a previous study (Fang *et al*., 2005), the Flame Luminosity Parameter can be defined as the ratio of the average flame luminosity over the released heat for the main injection. The Flame Luminosity Parameters (FLPs) are shown in Figure 6. A lower FLP value indicates lower sooting or lower combustion temperature. If the soot concentration and temperature are similar, a lower FLP value also indicates higher combustion efficiency. Lower values indicate better combustion performance for that injection event. From the results, it is apparent that higher injection pressure benefits the combustion performance. Earlier first injection timing also greatly influences the value of FLP. A combination of high injection pressure and earlier first injection timing with small fuel quantity results in a PCCI combustion process with the best performance.

4.3. Flame Spatial Fluctuation (FSF) and Flame Non-homogeneity (FNH)

Based on the definitions of FSF and FNH (Fang *et al*., 2005), both parameters were computed for all the cases. For each case, 5 sets of combustion images were used to obtain an averaged value. For completeness, the definitions of the two parameters are also listed below. The first parameter is defined as the Flame Spatial Fluctuation (FSF) as follows:

$$FSF = \sqrt{\sum_i \sum_j (I_{i,j} - \bar{I})^2} \quad (1)$$

where $I_{i,j}$ is the captured flame radiation intensity at pixel position (i, j) and $\bar{I}$ is the mean flame radiation intensity for an image at a certain crank angle. The flame non-homogeneity (FNH) is defined as the sum of the length of

spatial gradients for the images over all of the pixels:

$$FNH=\sum_i\sum_j \sqrt{\left(\frac{\partial I}{\partial x}\right)^2_{i,j}+\left(\frac{\partial I}{\partial y}\right)^2_{i,j}} \quad (2)$$

where $\partial I/\partial x$ and $\partial I/\partial Y$ are the partial differentiation in the x and y direction, respectively. The difference in these two parameters has been discussed by Fang *et al.* (2005). The FSF and FNH for the eight cases are plotted in Figures 7 and 8, respectively.

Figure 7 shows that the diffusion dominant combustion process has higher FSF values, showing highly substantial fluctuations in flame spatial distributions. It is also noted that the high injection pressure diffusion combustion cases, namely Cases 6 and 8, have slightly higher FSF values, indicating that high injection pressure might lead to a more fluctuating diffusion flame. On the other hand, the premixed dominant combustion process has lower FSF values due to a more uniform flame distribution for the cases such as Case 5 and Case 7. Compared with flame luminosity, the FSF peak timing is later than the flame luminosity peak timing, which shows that high flame luminosity does not imply high flame fluctuation or non-uniformity. The reason for this can be explained as follows by referencing the combustion images in a later section. It has been shown previously (Mathews *et al*., 2003) that for multiple injection strategies, the combustion flame fills the entire combustion chamber, including the squish region at the early stage of combustion, and the late cycle combustion flame is mainly in the bowl region. The same observation can be seen in the combustion images discussed in the following section. At an early stage, flame fills the whole field of view, which will lead to a higher value of flame luminosity by summing up the pixel values. But for FSF, a more distributed flame structure results in a smaller value. With continued combustion, the flame is more concentrated in the bowl region and has a donut shape structure. Although the flame luminosity is reduced at this time, a more concentrated high flame intensity donut shaped region leads to a larger value of FSF. Such a characteristic of the flame development process can be clearly illustrated by the defined FSF.

The FNH time histories for the eight cases are depicted in Figure 8. Trends similar to the FSF can be seen for different injection parameters. Higher injection pressures lead to lower FNH values. The diffusion dominant combustion cases have higher FNH values, indicating more heterogeneity, while premixed dominant combustion cases have lower values, which indicates more homogeneous combustion. An obvious difference of FNH from FSF is the peak timing. It can be seen that the FNH peak timing is often earlier than the FSF peak timing. Compared with the flame luminosity results, it is seen that the FNH peak timing is close to the flame luminosity peak timing. The peaks of FNH are mainly due to the jet structure or flame edges in the combustion images. The combination of flame local intensity and jet structure determined the FNH values. Because the later cycle combustion has no jet structure, the FNH value will be reduced for late cycle combustion.

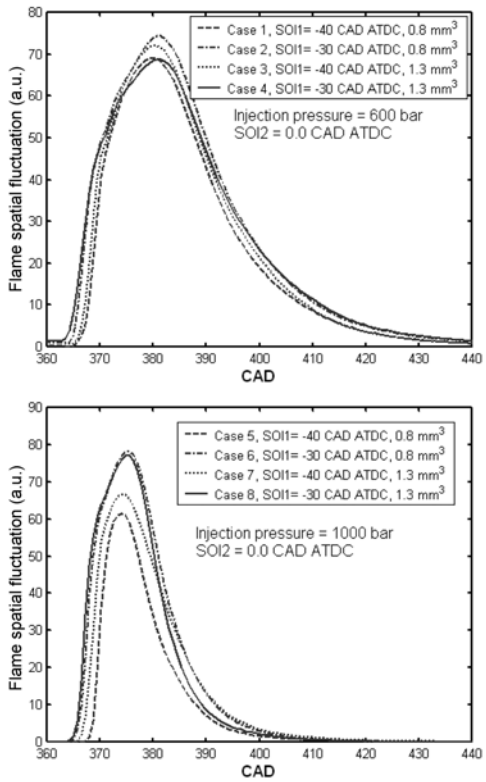

Figure 7. FSF time history for the eight cases.

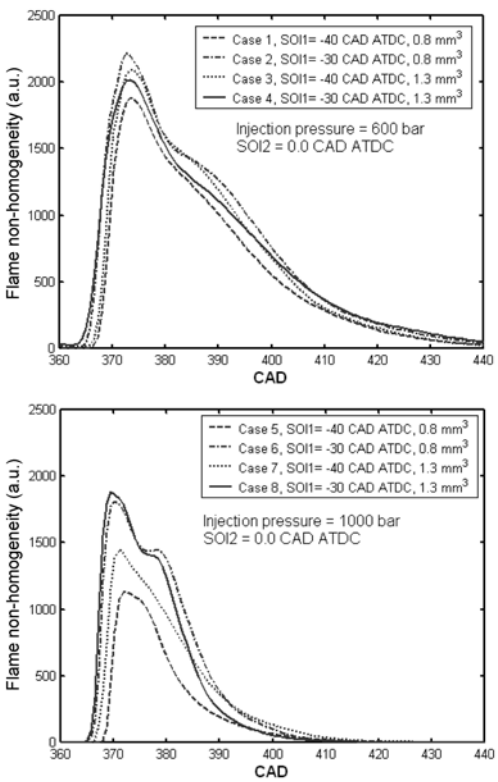

Figure 8. FNH time history for the eight cases.

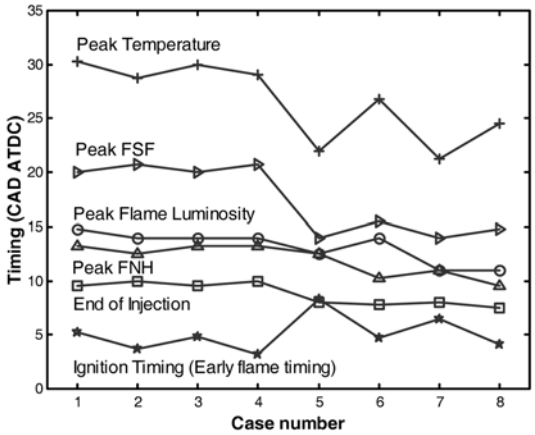

Figure 9. Some critical timings for the eight cases.

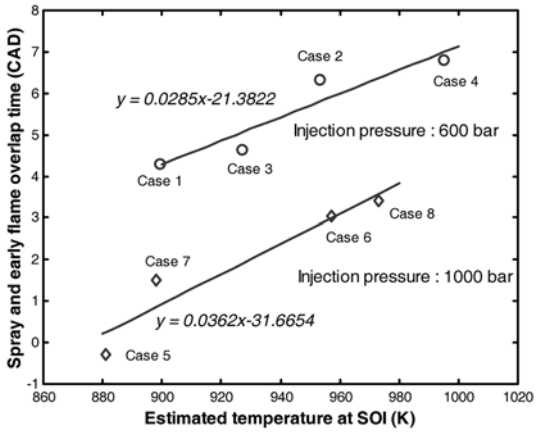

Figure 10. Liquid spray and early flame overlap time versus estimated in-cylinder temperature at SOI for the eight cases.

Premixed combustion has little jet structure as well as low flame intensity, and therefore has a lower value of FNH.

Based on the above discussions, some characteristic timings can be found from the time histories of the discussed parameters, as shown in Figure 9. Because the relationships of the peak flame luminosity timing with the peak FSF and FNH timings have been discussed before, this study will focus on other timings. One interesting timing difference is between the peak estimated in-cylinder temperature timing and the peak flame luminosity timing. It is found that the peak flame luminosity timing is always earlier than the peak bulk temperature timing, where the reason is that the in-cylinder bulk temperature depends mainly on the heat release process and expansion work. Heat is still being released during the soot oxidation process, and the in-cylinder temperature can increase as long as the expansion work is less than the heat release, which is often the case at the early stage of expansion. On the other hand, the flame luminosity is determined by temperature and soot concentration. Under similar local temperatures, flame luminosity peaks often occur at the highest soot concentration, with the soot formation rate balanced by the soot oxidation rate. When the soot oxidation rate is higher than the formation rate, flame luminosity will be reduced. Therefore, the peak in-cylinder temperature often occurs later than the peak flame luminosity timing.

Another important timing difference is the end of injection timing and the timing of early flame appearance. The difference of these two timings gives an overlap time, which might determine the combustion mode. If the overlap time is less than zero, there will be purely premixed combustion. Otherwise, the combustion mode will be some kind of diffusion flame. The overlap times of liquid spray and early flame are illustrated in Figure 10 for the eight cases. The results are grouped into two categories, including a lower injection pressure group and a higher injection pressure group. The data points were also fitted with a straight line to estimate the variation trend. It is seen that lower injection pressure results in a larger value of overlap time, and all the overlap times are positive for these cases, which indicates diffusion flame combustion. However, for higher injection pressure the overlap time is smaller and is even negative for Case 5, leading to premixed combustion. The overlap time increases with ambient temperature at the start of the second injection for both injection pressures. The ambient temperature is mainly dependent on the parameters of the first injection. An earlier first injection with small fuel quantity using higher injection pressure is preferable for obtaining PCCI combustion. Another approach is to retard the second injection timing after TDC with a lower SOI temperature, which is used in UNIBUS combustion (Hasegawa and Yanagihara, 2003).

4.4. Combustion Images

The digital combustion images obtained using the high-speed video camera were processed using the same color-map and scales to compare different injection parameters. The camera was operated at 12000 frames per second. This frame rate corresponds to 0.75 CAD intervals between two sequential images at 1500 rpm. For each case, 5 combustion movies were taken and a typical whole cycle movie

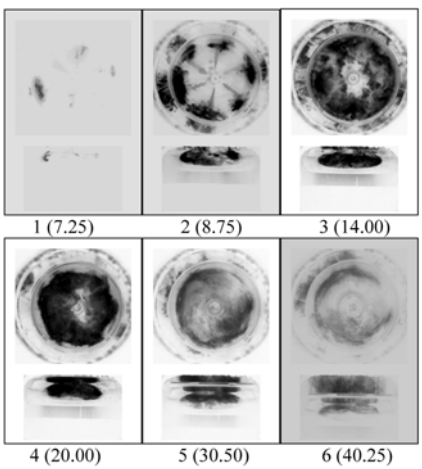

Figure 11. Combustion images Case 1. All times shown in CAD ASOI in the brackets.

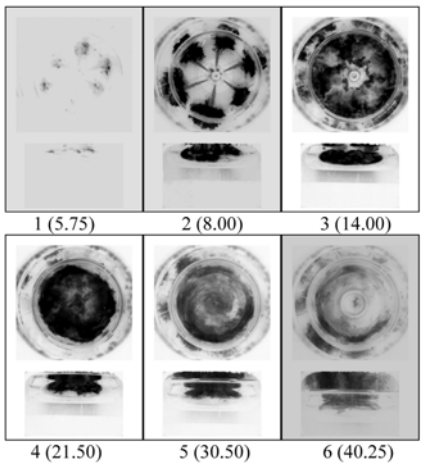

Figure 12. Combustion images Case 2. All times shown in CAD ASOI in the brackets.

was selected for analysis and presentation. For each set of combustion images, 6 images are presented to show the combustion flames at different times, including two early flame images (the first two images), one at peak flame luminosity timing (the third), one at peak FSF timing (the 4th), and two late cycle flame images (the 5th and 6th). In order to enhance the image contrast, the contrast factor for the first two images and the sixth image were adjusted when presenting them in the figures.

The combustion images for the eight cases are shown in Figures 11~18, respectively. The first two images in each figure show the ignition points and early flame developments. The ignition processes are consistent with the pressure and heat release rate results. For most of the cases, the ignition points are located in the bowl region near the spray tip areas. From the side window images, it is found that the early flame pockets are located in the near wall region of the bowl. However, for Cases 2 and 4, the ignition points are located more upstream than in the other cases because of high ambient temperature at the start of

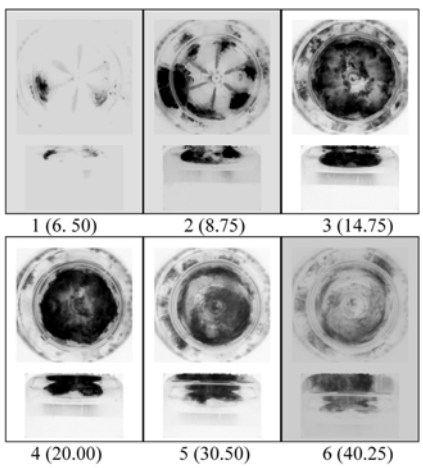

Figure 13. Combustion images Case 3. All times shown in CAD ASOI in the brackets.

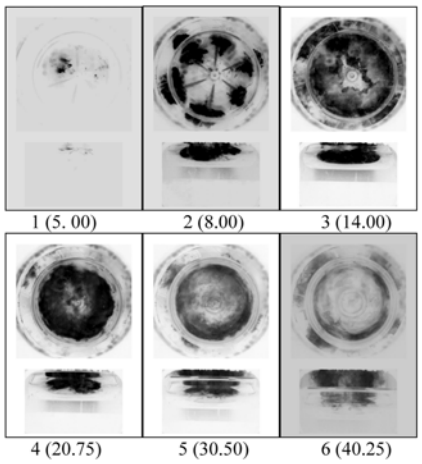

Figure 14. Combustion images Case 4. All times shown in CAD ASOI in the brackets.

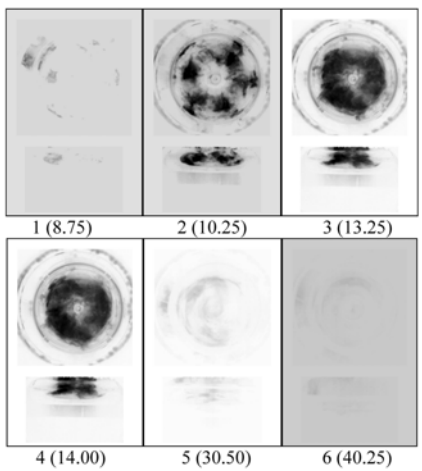

Figure 15. Combustion images Case 5. All times shown in CAD ASOI in the brackets.

injection. This is consistent with previous work with different injection pressures for conventional diffusion combustion (Minami *et al*., 1990). Higher first injection fuel quantity and later first injection timing lead to earlier appearances of the flame points in the combustion chamber.

Diffusion flame combustion is clearly seen for all of the low injection pressure cases and for Cases 6 and 8, with liquid fuel being injected into hot flame. Some evidence can also be seen for Case 7. However, an apparent premixed combustion is seen for Case 5. Lower injection pressure cases have stronger diffusion flames than the higher injection pressure cases. The strength of the diffusion flame correlates well with the ambient temperature at the start of the second injection. Therefore, the factor resulting in a higher ambient temperature at the start of second injection leads to a stronger diffusion flame. Higher first fuel quantity and later injection timing cause stronger diffusion flames.

For most of the cases, the flame fills the squish region. However, little flame is seen in the squish region for Cases

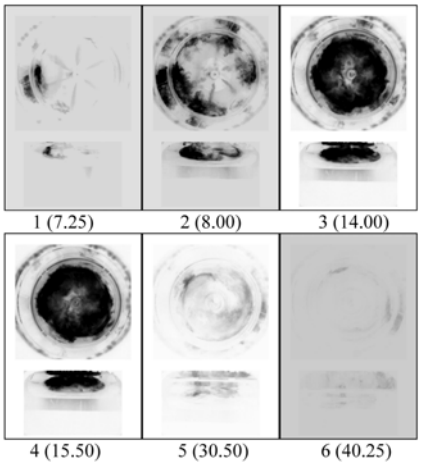

Figure 16. Combustion images Case 6. All times shown in CAD ASOI in the brackets.

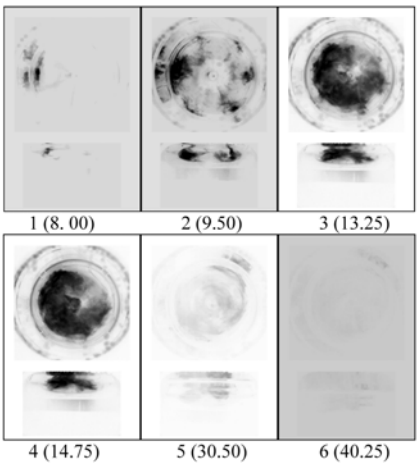

Figure 17. Combustion images Case 7. All times shown in CAD ASOI in the brackets.

5 and 7; most of the flame is in the bowl region, even in the early stage of combustion. In the late combustion period, most of the flame is in the bowl region with a donut shape due to the strong swirling motion in the combustion chamber.

For the combustion images at peak flame luminosity timing, namely the third image, large differences can be seen for differing injection pressure cases. For the low injection pressure cases, the flame is more widespread than in the higher injection pressure cases. Most of the higher injection pressure flame is concentrated in the bowl region. For images at the peak FSF value timings, the flame is similar for all of the cases and has a donut shape. It is more concentrated in a circular region between the injector tip and bowl wall. This clearly explains why the peak flame luminosity timing is earlier than the peak FSF timing, as mentioned previously. For the higher injection pressure cases, the difference between these two timings becomes smaller because both timings have similar flame structures for most of the cases except Case 8.

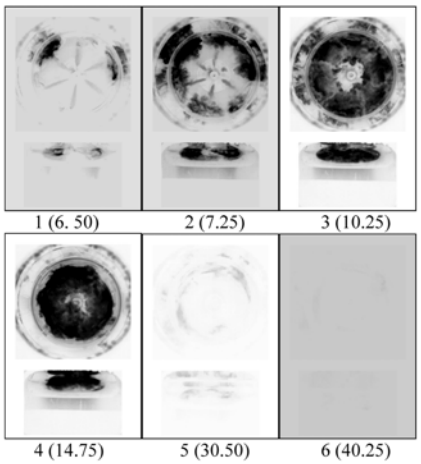

Figure 18. Combustion images Case 8. All times shown in CAD ASOI in the brackets.

From the late cycle combustion images (the fifth and sixth images), much weaker late cycle flame intensity is seen in the higher injection pressure cases. High injection pressure results in a higher soot oxidation rate under similar conditions. This higher soot oxidation rate can be attributed to a higher combustion temperature under higher injection pressure (Kobayashi *et al.*, 1992). A fast soot oxidation rate results in less soot going out to the exhaust.

5. CONCLUSIONS

In the current work, the influences of the injection parameters on the combustion mode transition were investigated. The effects of injection timing, injection fuel quantity, and injection pressure were discussed. Several parameters were defined and used to evaluate the flame structure and combustion performance. Some observations and conclusions are listed as follows:

The first injection parameters affect the ambient environment at the start of the second injection event and influence the combustion mode for the second injection. Higher second injection SOI temperatures are seen for higher first injection fuel quantities, later first injection timing, and lower injection pressures. The SOI temperature greatly influences the spray and flame overlap time, which directly determines the combustion mode.

A small fuel quantity, early injection timing of the first injection event, and high injection pressure are preferable for low sooting and/or low temperature combustion;

Combustion visualization results show the transition from PCCI combustion mode to conventional diesel combustion mode. The diffusion flame fills the whole combustion chamber, while for the PCCI mode most flame is confined in the bowl region. Late cycle flames are in the bowl region for both combustion modes;

Newly defined parameters, such as FSF and FNH, provide further insights into the combustion structure and flame development process.

ACKNOWLEDGEMENT–This work was supported in part by the Department of Energy Grant No. DE-FC26-05NT42634, by Department of Energy GATE Centers of Excellence Grant No. DE-FG26-05NT42622, and by the Ford Motor Company under University Research Program. We also thank Paul Miles of Sandia National Laboratories, Evangelos Karvounis and Werner Willems of Ford for their assistance on the design of the optical engine and on the setup of the experiments.

REFERENCES

Akagawa, H., Miyamoto, T., Harada, A., Sasaki, S., Shimazaki, N., Hashizume, T. and Tsujimura, K. (1999). Approaches to solve problems of the premixed lean diesel combustion. *SAE Paper No.* 1999-01-0183.

Chen, S. K. (2000). Simultaneous reduction of NOx and particulate emissions by using multiple injections in a small diesel engine. *SAE Paper No.* 2000-01-3084.

Choi, G. H., Han, S. B. and Dibble, R. W. (2004). Experiental study on homogeneous charge compression ignition engine operation with exhaust gas recirculation. *Int. J. Automotive Technology* **5**, **3**, 195–200.

Fang, T., Coverdill, R. E., Lee, C. F. and White, R. A. (2005). Low temperature combustion within a small-bore high-speed direct-injection (HSDI) diesel engine. *SAE Paper No.* 2005-01-0919.

Fang, T., Coverdill, R. E., Lee, C. F. and White, R. A. (2006). Combustion and soot visualization of low temperature combustion within an HSDI diesel engine using multiple injection strategy. *SAE Paper No.* 2006-01-0078.

Fang, T., Coverdill, R. E., Lee, C. F. and White, R. A. (2007). Smokeless combustion within a small-bore HSDI diesel engine using a narrow angle injector. *SAE Paper No.* 2007-01-0203*, SAE Trans.: J. Engines*, **116**, Section 3, 255–270.

Fang, T., Coverdill, R. E., Lee, C. F. and White, R. A. (2008). Effects of injection angles on combustion processes using multiple injection strategies in an HSDI diesel engine. *Fuel* **87**, **15/16**, 3232–3239.

Han, Z., Uludogan, A., Hampson, G. J. and Reitz, R. D. (1996). Mechanism of soot and NOx emission reduction using multiple injection in a diesel engine. *SAE Paper No.* 960633.

Hasegawa, R. and Yanagihara, Y. (2003). HCCI combustion in DI diesel engine. *SAE Paper No.* 2003-01-0745.

Hashizume, T., Miyamoto, T., Akagawa, H. and Tsujimura, K. (1998). Combustion and emission characteristics of multiple stage diesel combustion. *SAE Paper No.* 980505.

Helmantel, A. and Denbratt, I. (2004). HCCI operation of a passenger car common rail DI diesel engine with early injection of conventional diesel fuel. *SAE Paper No.* 2004-01-0935.

Kobayashi, S., Sakai, T., Nakahira, T., Komori, M. and Tsujimura, K. (1992). Measuremnt of flame temperature distribution in DI diesel engine with high pressure fuel injection. *SAE Paper No.* 920692.

Kook, S. and Bae C. (2004). Combustion control using two-stage diesel fuel injection in a single cylinder PCCI engine. *SAE Paper No.* 2004-01-0938.

Mathews, W. S., Coverdill, R. E., Lee, C. F. and White, R. A. (2002). Liquid and vapor fuel distributions in a small-bore high-speed direct-injection diesel engine. *SAE Paper No.* 2002-01-0266.

Mathews, W. S., Fang, T., Coverdill, R. E., Lee, C. F. and White, R. A. (2003). Combustion visualization of multiple injections within an HSDI diesel engine. *Proc. 3rd Joint Meeting of the US Sections of the Combustion Institute*, Chicago, IL.

Miles, P. C. (2000). The Influence of swirl on HSDI diesel combustion at moderate speed and load. *SAE Paper No.* 2000-01-1829.

Minami, T., Yamaguchi, I., Shintani, M., Tsujimura, K. and Suzuki, T. (1990). Analysis of fuel spray characteristics and combustion phenomena under high pressure fuel injection. *SAE Paper No.* 900438.

Najt, P. M. and Foster, D. E. (1983). Compression ignition homogeneous charge combustion. *SAE Paper No.* 830264.

Nehmer, D. A. and Reitz, R. D. (1994). Measurement of the effect of injection rate and split injections on diesel engine soot and NOx emissions. *SAE Paper No.* 940668.

Noguchi, M., Tanaka, Y., Tanaka, T. and Takeuchi, Y. (1979). A study on gasoline engine combustion by observation of intermediate reactive products during combustion. *SAE Paper No.* 790840.

Onishi, S., Hong Jo, S., Shoda, K., Do Jo, P. and Kato, S. (1979). Active thermo-atmosphere combustion (ATAC) - A new combustion process for internal combustion engines. *SAE Paper No.* 790501.

Su, W., Lin, T. and Pei, Y. (2003). A compound technology for HCCI combustion in a DI diesel engine with early injection of conventional diesel fuel. *SAE Paper No.* 2003-01-0741.

Swami Nathan, S., Mallikarjuna, J. M. and Ramesh, A. (2007). Effect of mixture preparation in a diesel HCCI engine using early in-cylinder injection during the suction stroke. *Int. J. Automotive Technology* **8**, **5**, 543–553.

Takeda, Y., Keiichi, N. and Keiichi, N. (1996). Emission characteristics of premixed lean diesel combustion with extremely early staged fuel injection. *SAE Paper No.* 961163.

Tanaka, T., Ando, A. and Ishizaka, K. (2002). Study on pilot injection of DI diesel engine using common rail injection system. *JSAE Review*, **23**, 297–302.

Thring, R. H. (1989). Homogeneous charge compression ignition (HCCI) engine. *SAE Paper No.* 892068.

Tow, T. C., Pierpont, D. A. and Reitz, R. D. (1994). Reducing particulate and NOx emissions by using multiple injections in a heady duty DI diesel engine. *SAE Paper No.* 940897.

Van Gerpen, J. H., Huang, C. W. and Borman, G. L. (1985). The effects of swirl and injection parameters on diesel combustion and heat transfer. *SAE Paper No.* 850265.

Zhang, L. (1999). A study of pilot injection in a DI diesel engine. *SAE Paper No.* 1999-01-3493.